Detection of Gamma-Ray Emission from the Vela Pulsar Wind Nebula with AGILE

A. Pellizzoni,[1]* A. Trois,[2] M. Tavani,[2,3,4,5] M. Pilia,[1,6] A. Giuliani,[7] G. Pucella,[8] P. Esposito,[7,9] S. Sabatini,[2,4] G. Piano,[2,4] A. Argan,[2] G. Barbiellini,[10] A. Bulgarelli,[11] M. Burgay,[1] P. Caraveo,[7] P. W. Cattaneo,[9] A. W. Chen,[7] V. Cocco,[2] T. Contessi,[7] E. Costa,[2] F. D'Ammando,[2,3] E. Del Monte,[2] G. De Paris,[2] G. Di Cocco,[2] G. Di Persio,[2] I. Donnarumma,[2] Y. Evangelista,[2] M. Feroci,[2] A. Ferrari,[5] M. Fiorini,[7] F. Fuschino,[11] M. Galli,[12] F. Gianotti,[11] A. Hotan,[13] C. Labanti,[11] I. Lapshov,[2] F. Lazzarotto,[2] P. Lipari,[14] F. Longo,[10] M. Marisaldi,[11] M. Mastropietro,[2] S. Mereghetti,[7] E. Moretti,[10] A. Morselli,[4] L. Pacciani,[2] J. Palfreyman,[15] F. Perotti,[7] P. Picozza,[3,4] C. Pittori,[16] A. Possenti,[1] M. Prest,[6] M. Rapisarda,[8] A. Rappoldi,[9] E. Rossi,[11] A. Rubini,[2] P. Santolamazza,[16] E. Scalise,[2] P. Soffitta,[2] E. Striani,[3,4] M. Trifoglio,[11] E. Vallazza,[10] S. Vercellone,[17] F. Verrecchia,[16] V. Vittorini,[3] A. Zambra,[7] D. Zanello,[14] P. Giommi,[16] S. Colafrancesco,[16] A. Antonelli,[16] L. Salotti,[18] N. D'Amico,[1,19] G. F. Bignami[20]

Pulsars are known to power winds of relativistic particles that can produce bright nebulae by interacting with the surrounding medium. These pulsar wind nebulae are observed by their radio, optical, and x-ray emissions, and in some cases also at TeV (teraelectron volt) energies, but the lack of information in the gamma-ray band precludes drawing a comprehensive multiwavelength picture of their phenomenology and emission mechanisms. Using data from the AGILE satellite, we detected the Vela pulsar wind nebula in the energy range from 100 MeV to 3 GeV. This result constrains the particle population responsible for the GeV emission and establishes a class of gamma-ray emitters that could account for a fraction of the unidentified galactic gamma-ray sources.

The Vela supernova remnant (SNR) is the nearest SNR (distance ≈ 290 pc) containing a bright pulsar, PSR B0833-45, which has a characteristic age of 11,000 years and a spin-down luminosity of 7×10^{36} erg s^{-1} (*1*, *2*). This SNR extends over a diameter of ~8° and is known from early radio observations to embrace a number of regions of nonthermal emission (*3*) including Vela X, a flat-spectrum radio component with a diameter of 100 arc min near the center of the SNR. Vela X, separated from PSR B0833-45 by ~40 arc min, is generally interpreted as the pulsar's radio synchrotron nebula (*4*, *5*). A diffuse emission feature (~1° long) coincident with the center of Vela X was detected in x-rays (0.6 to 7.0 keV) by the Röntgen (*6*) and ASCA (*7*) satellites. It was first suggested that this feature, which is closely aligned with a filament detected at radio wavelengths, corresponds to the outflow jet from the pulsar's pole (*8*). More recently, observations with Chandra (*9*) clearly unveiled the torus-like morphology of the compact x-ray nebula surrounding the pulsar and indicated that the center of Vela X lies along the extension of the pulsar equator, although bending to the southwest.

The detection of very-high-energy (VHE; 0.5 to 70 TeV) gamma rays from the Vela X region was claimed by HESS (*10*) and confirmed by CANGAROO (*11*). The strong VHE source HESS J0835-455 (luminosity $\sim 10^{33}$ erg s^{-1} at energies above 0.55 TeV) coincides with the region of hard x-ray emission seen by the Röntgen satellite. The best-fit VHE emission centroid (RA = $08^{h}35^{m}1^{s}$, Dec = −45°34′40″) is ~0.5° from the pulsar position, and the VHE emission has an extension of ~5 parsec × 4 parsec. The detection of Vela X at TeV energies demonstrated that this source emits nonthermal radiation, in agreement with the hypothesis that it corresponds to the pulsar wind nebula (PWN), displaced to the south by the unequal pressure of the reverse shock from the SNR (*12*).

The multiwavelength spectrum of the center of Vela X can be modeled as synchrotron radiation from energetic electrons within the cocoon (radio and x-rays) and inverse-Compton (IC) emission from the scattering (by the same electron population) of the cosmic microwave background radiation (CMBR), the galactic far-infrared radiation (FIR) produced by reradiation of dust grains, and the local starlight (*13*–*15*). Alternatively, a hadronic model can be invoked for the gamma-ray emission from the Vela X cocoon, where the emission is the result of the decay of neutral pions produced in proton-proton collisions (*16*). Observations in the high-energy (HE) MeV-GeV band are crucial to distinguish between leptonic and hadronic models as well as to identify specific particle populations and spectra.

The Vela region was recently observed from 30 MeV to 50 GeV by the AGILE (*17*) and Fermi (*18*) gamma-ray satellites. The Vela pulsar is the brightest persistent source of the GeV sky, and, because of the limited angular resolution of the current-generation gamma-ray instruments, its gamma-ray pulsed emission dominates the surrounding region up to a radius of ~5°, preventing the effective identification of weaker nearby sources.

The AGILE satellite (*19*) observed the Vela pulsar for ~180 days (within 60° from the center of instrument's field of view) from July 2007 [54294.5 MJD (modified Julian day)] to September 2009 (55077.7 MJD). To obtain precise radio ephemeris and to model the Vela pulsar timing noise for the entire AGILE data span, we made use of observations with the Mount Pleasant radio telescope (see supporting online material). The Vela pulsar timing analysis provided a total of ~40,000 pulsed counts with energies between 30 MeV and 50 GeV; the difference between the radio and gamma-ray ephemeris was $<10^{-11}$ s. Gamma-ray pulsed counts are concentrated within the phase interval 0.05 to 0.65 (where 0 is the phase corresponding to the main radio peak; see fig. S1). We verified that no pulsed gamma-ray emission is detected outside this interval, consistent with reports of previous observations by EGRET (*20*, *21*), AGILE (*17*), and Fermi (*18*).

With the aim of performing a sensitive search for close faint sources excluding the bright emission from the Vela pulsar, we discarded the time intervals corresponding to the phase interval 0.05 to 0.65. The analysis of the resulting off-pulse images (taking only events corresponding to the pulsar phase interval 0.65 to 1.05, for a total of ~14,000 events) unveiled few gamma-ray sources, none of which coincides with the Vela pulsar. A maximum likelihood analysis (*19*), performed on the E (energy) > 100 MeV data set within a region of 5° around the pulsar position, revealed two sources at better than 3σ confidence (Fig. 1 and fig. S2): AGL J0848-4242 [at galactic coordinates l = 263.11°, b = 0.65°, 68%

[1]INAF–Osservatorio Astronomico di Cagliari, loc. Poggio dei Pini, strada 54, I-09012, Capoterra (CA), Italy. [2]INAF-IASF Roma, via del Fosso del Cavaliere 100, I-00133 Roma, Italy. [3]Dipartimento di Fisica, Università Tor Vergata, via della Ricerca Scientifica 1, I-00133 Roma, Italy. [4]INFN-Roma Tor Vergata, via della Ricerca Scientifica 1, I-00133 Roma, Italy. [5]Consorzio Interuniversitario per la Fisica Spaziale, viale Settimio Severo 63, I-10133 Torino, Italy. [6]Dipartimento di Fisica, Università dell'Insubria, via Valleggio 11, I-22100 Como, Italy. [7]INAF-IASF Milano, via E. Bassini 15, I-20133 Milano, Italy. [8]ENEA Frascati, via E. Fermi 45, I-00044 Frascati (Roma), Italy. [9]INFN-Pavia, via A. Bassi 6, I-27100 Pavia, Italy. [10]INFN-Trieste, Padriciano 99, I-34012 Trieste, Italy. [11]INAF-IASF Bologna, via P. Gobetti 101, I-40129 Bologna, Italy. [12]ENEA Bologna, via don G. Fiammelli 2, I-40128 Bologna, Italy. [13]Curtin University of Technology, 78 Murray Street, Perth, WA 6000, Australia. [14]INFN-Roma La Sapienza, p.le A. Moro 2, I-00185 Roma, Italy. [15]School of Mathematics and Physics, University of Tasmania, Hobart, TAS 7001, Australia. [16]ASI Science Data Center, ESRIN, I-00044 Frascati (Roma), Italy. [17]INAF-IASF Palermo, via U. La Malfa 153, I-90146 Palermo, Italy. [18]ASI–Agenzia Spaziale Italiana, viale Liegi 26, I-00198 Roma, Italy. [19]Dipartimento di Fisica, Università di Cagliari, Cittadella Universitaria, I-09042 Monserrato (CA), Italy. [20]Istituto Universitario di Studi Superiori, viale Lungo Ticino Sforza 56, I-27100 Pavia, Italy.

*To whom correspondence should be addressed. E-mail: apellizz@ca.astro.it

confidence error circle (e.c.) radius ~0.25°] and AGL J0834-4539 (at $l = 263.88°$, $b = -3.17°$, e.c. radius ~0.20°). A gamma-ray source coincident with the EGRET source 3EG J0841-4356 (*22*) was also detected with lower significance, and the Vela Junior (RX J0852.0-4622) SNR (*23*, *24*) also possibly contributes to an excess of counts in the galactic plane around $l \approx 265.6°$.

The brightest gamma-ray source, AGL J0834-4539 [~5.9σ significance, ~264 counts, photon flux $F\gamma = 35 \times 10^{-8}$ ($\pm 7 \times 10^{-8}$) photons cm^{-2} s^{-1} at $E > 100$ MeV], is located ~0.5° southwest from the Vela pulsar position (outside the 95% source position confidence contour) and has a spatial extent of ~1.5° × 1°. Its shape is asymmetric and incompatible with the AGILE point-spread function. Therefore, possible residual emission from the pulsar (in principle associated to undetected weak peaks in the off-pulse interval of the light curve) cannot substantially contribute to this diffuse feature. No relevant systematic errors on positions, fluxes, and spectra (mostly due to uncertainties on the galactic gamma-ray diffuse emission model) affect AGILE sources detected around the 5σ level (see supporting online material). AGL J0834-4539 is positionally coincident with HESS J0835-455, the TeV source that is identified with the Vela X nebula, and has a similar brightness profile to it (Fig. 1). This implies that AGL J0834-4539 is associated with the pulsar's PWN.

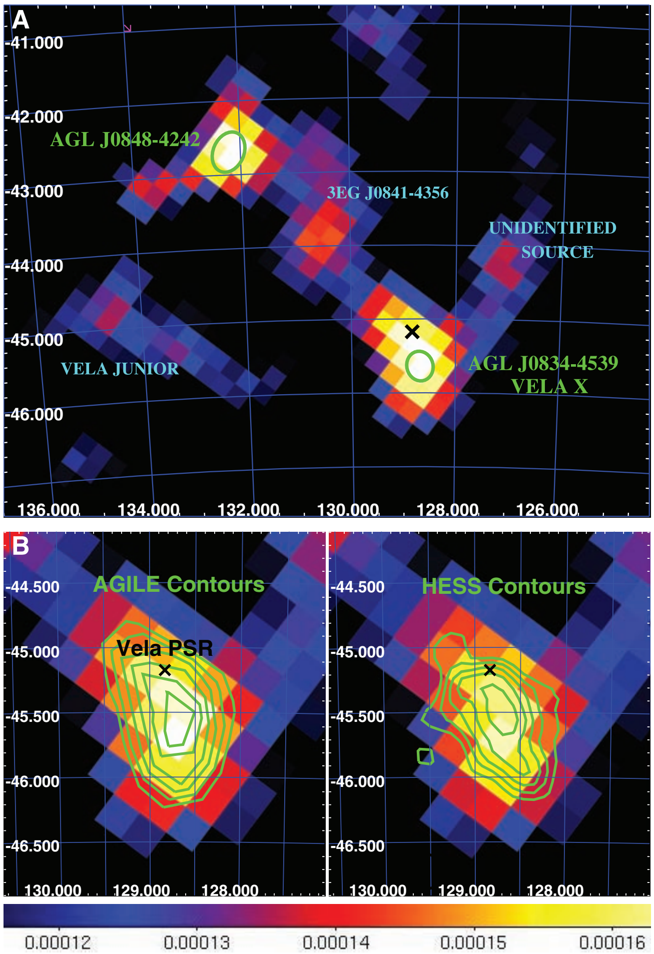

Fig. 1. (**A**) Gaussian-smoothed AGILE intensity map (photons cm^{-2} s^{-1} sr^{-1} with pixel size 0.25° × 0.25°) at $E > 400$ MeV around the Vela pulsar, including only off-pulse events (i.e., discarding events with phase corresponding to Vela pulsed emission). The neutron star position is marked with a black cross; green circles are the 68% confidence contours for the position of AGL J0848-4242 and AGL J0834-4539 (Vela X). The AGILE $E > 400$ MeV energy band is well suited for gamma-ray imaging and provides a good compromise between the instrument-effective area (~400 cm^2; ~100 counts from AGL J0834-4539) and point-spread function (~1°, 68% containment radius), both parameters decreasing with energy. (**B**) The gamma-ray diffuse source AGL J0834-4539. AGILE contours (left) are in the range 1.4×10^{-4} to 1.6×10^{-4} photons cm^{-2} s^{-1} sr^{-1}, with step 4×10^{-6}. HESS contours (right) are from (*10*).

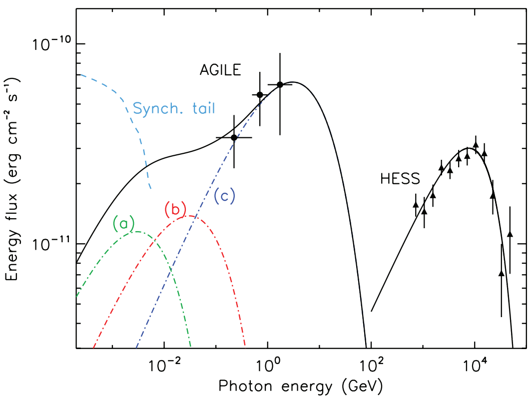

Fig. 2. Gamma-ray high-energy and very-high-energy νF_ν spectrum of the Vela X PWN. HESS data fit an IC process (scattering on CMBR) related to electron power-law index 2.0 with a break at 67 TeV and a total energy content of 2.2×10^{45} erg (*10*). AGILE data are compatible with IC emission from the additional electron component, well reproducing the observed total radio spectrum ($E_{tot} = 4 \times 10^{48}$ erg), assuming the same field strength (~5 μG) as required by the TeV spectral break. Unlike the TeV IC emission, GeV IC scattering is within the Thomson limit. Thus, in addition to the CMBR component (photon density $n_{ph} = 0.25$ eV cm^{-3}, photon energy $E_{ph} = 10^{-3}$ eV), also FIR ($n_{ph} = 0.3$ eV cm^{-3}, $E_{ph} = 10^{-2}$ eV) and starlight ($n_{ph} = 1.4$ eV cm^{-3}, $E_{ph} = 1$ eV) photon fields can significantly contribute to the high-energy IC counterpart of the radio spectrum fitting AGILE data [dot-dashed lines: CMBR (a), FIR (b), starlight (c); thick line: total IC spectrum].

On the basis of the available count statistics, we performed a first estimate of the spectrum by sampling the flux in the three energy bands (0.1 to 0.5 GeV, 0.5 to 1 GeV, and 1 to 3 GeV; Fig. 2) where the source is clearly detected. A power-law fit yields a photon index $\alpha = -1.67 \pm 0.25$. The AGILE spectral points are a factor of ~2 below the previous EGRET upper limits (*25*) and well above the extrapolation of the HESS spectral energy distribution νF_ν to lower energies. The PWN gamma-ray luminosity in the 0.1- to 10-GeV band, for a distance of ~290 pc (*2*, *26*), is $4^{+4}_{-2} \times 10^{33}$ erg s^{-1}, corresponding to $\sim 10^{-3}\,\dot{E}_{rot}$ (where $\dot{E}_{rot}$ is the spin-down luminosity of the pulsar). Such a luminosity is slightly higher than at VHE energies (9.9×10^{32} erg s^{-1}).

In the frame of leptonic models, the AGILE measurements are not consistent with a simple multiwavelength spectral energy distribution involving a single electron population. The AGILE spectral points are one order of magnitude above the fluxes expected from the electron population simultaneously fitting synchrotron x-ray emission (peaking at ~1 keV) and IC TeV emission (*10*, *14*).

Additional electron populations should be invoked to explain the observed GeV fluxes. This is not surprising in view of the complex morphology of the PWN seen in radio and x-rays, where different sites and features of nonthermal emission are present: The anisotropic pulsar wind and nonhomogeneous SNR reverse shock pressure produce different particle populations within the shocked wind. In particular, assuming the same magnetic field (5 μG) reproducing the TeV spectral break, the radio synchrotron emitting electrons observed in the Vela X structure (*27*) may be responsible for the IC bump in the GeV band arising from scattering on CMBR and galactic and starlight photon fields, as predicted by de Jager *et al.* (*13*, *15*). Indeed, the position where AGILE sees the maximum brightness (RA = 08^{h}35^m, Dec = −45°44′) is also roughly where the 8.4-GHz radio emission is brightest (*28*). AGILE data are compatible with the IC parameters modeled by de Jager *et al.* (*15*) (electron spectral index 1.78 and maximum energy ~20 GeV), although our measurements could suggest a higher contribution from IC photon seeds. In particular, assuming a starlight energy density of 1.4 eV cm^{-3} and a mean temperature of ~2300 K (*29*), we obtain a good description of the AGILE data (Fig. 2).

The AGILE measurements would be incompatible with the scenario of nucleonic gamma-ray production in the Vela TeV nebula in the frame of a single primary electron population. These models predict very faint GeV emission ($<10^{30}$ erg s^{-1}) even when including synchrotron and IC emission from primary and secondary electrons produced by the inelastic nuclear scattering (*16*). On the other hand, the proposed additional electron component scenario described above leaves room for uncorrelated GeV-TeV emission, although the comprehensive multiwavelength two-component leptonic model (providing strong IC emission on a relatively dense photon field) seems to disfavor dominant nucleonic gamma-ray production. In fact, it has been found that the thermal particle density at the head of the cocoon, where bright VHE gamma-ray emission was found, is lower than that required by hadronic models by a factor of 6 (*14*).

The radio-emitting region mentioned above appears to be larger (~2° × 3°) than the AGILE nebula, possibly indicating that IC cooling in the GeV domain is important. However, the actual physical size of the GeV nebula could be larger than what we are able to resolve with the available photon statistics, because of the strong galactic gamma-ray emission affecting MeV-GeV energy bands. Instead, the AGILE nebula is similar in shape to the HESS nebula, which may suggest that the core of HE and VHE emission is produced in the same projected region of Vela X, even if different electron populations are involved. Indeed, different spots of bright radio emission (*28*), possibly associated to electrons injected at different stages of pulsar evolution, are embedded within the poorly resolved HE and VHE emission regions.

High-energy PWN emissions are thought to be a common phenomenon associated with young and energetic pulsars (*30*) because the IC emission of these PWNe arises mostly from scattering on CMBR and starlight fields, with no special environmental requirements. On the other hand, PWN emissions are expected to be much weaker than pulsed emission from the associated neutron star, especially in the GeV domain where most of the pulsar's spin-down energy is funneled. Indeed, despite a PWN gamma ray yield of $L_\gamma^{PWN} \approx 10^{-3} \times \dot{E}_{rot}$, to be compared with the typical gamma-ray pulsed luminosity of $L_\gamma^{pulsed} \approx 10^{-2}$ to $0.1 \times \dot{E}_{rot}$, our AGILE observation shows that 10,000-year-old PWNe can match the sensitivities of current GeV instruments.

Because the gamma-ray luminosity of the PWN is only a small fraction of the beamed emission from the neutron star, the PWN component is difficult to identify in weaker gamma-ray pulsars, although it could account for a substantial part of the observed off-pulse flux. However, if the beamed emission does not intersect the line of sight to the observer, the PWN component, unhindered by the stronger pulsed emission, could be detectable. Energetic pulsars (e.g., $\dot{E}_{rot} \approx 10^{37}$ erg s^{-1}) can power PWNe with gamma-ray luminosities matching the flux ($\sim10^{-8}$ to 10^{-7} photons cm^{-2} s^{-1}; $E > 100$ MeV) of a class of unidentified EGRET sources (*22*), as well as a subset of those detected by AGILE and Fermi (*31*, *32*), when placed within few kiloparsecs. The roughly isotropic emission from such undisturbed PWNe would not yield pulsations, and, as a class, they could contribute to the population of galactic unidentified sources still awaiting multiwavelength association (*13*, *33*).

References and Notes

1. J. H. Taylor, R. N. Manchester, A. G. Lyne, *Astrophys. J. Suppl. Ser.* **88**, 529 (1993).
2. R. Dodson, D. Legge, J. E. Reynolds, P. M. McCulloch, *Astrophys. J.* **596**, 1137 (2003).
3. H. Rishbeth, *Aust. J. Phys.* **11**, 550 (1958).
4. K. W. Weiler, N. Panagia, *Astron. Astrophys.* **90**, 269 (1980).
5. K. S. Dwarakanath, *J. Astrophys. Astron.* **12**, 199 (1991).
6. C. B. Markwardt, H. B. Oegelman, *Nature* **375**, 40 (1995).
7. C. B. Markwardt, H. B. Oegelman, *Astrophys. J.* **480**, 13 (1997).
8. D. A. Frail, M. F. Bietenholz, C. B. Markwardt, H. Oegelman, *Astrophys. J.* **475**, 224 (1997).
9. D. J. Helfand, E. V. Gotthelf, J. P. Halpern, *Astrophys. J.* **556**, 380 (2001).
10. F. Aharonian *et al.*, *Astron. Astrophys.* **448**, L43 (2006).
11. R. Enomoto *et al.*, *Astrophys. J.* **638**, 397 (2006).
12. J. M. Blondin, R. A. Chevalier, D. M. Frierson, *Astrophys. J.* **563**, 806 (2001).
13. O. C. de Jager, *Astrophys. J.* **658**, 1177 (2007).
14. S. LaMassa, P. O. Slane, O. C. de Jager, *Astrophys. J.* **689**, L121 (2008).
15. O. C. de Jager, P. O. Slane, S. LaMassa, *Astrophys. J.* **689**, L125 (2008).
16. D. Horns, F. Aharonian, A. Santangelo, A. I. D. Hoffmann, C. Masterson, *Astron. Astrophys.* **451**, L51 (2006).
17. A. Pellizzoni *et al.*, *Astrophys. J.* **691**, 1618 (2009).
18. A. Abdo *et al.*, *Astrophys. J.* **696**, 1084 (2009).
19. M. Tavani *et al.*, *Astron. Astrophys.* **502**, 995 (2009).
20. G. Kanbach *et al.*, *Astron. Astrophys.* **289**, 855 (1994).
21. D. J. Thompson, in *Cosmic Gamma-Ray Sources*, K. S. Cheng, G. E. Romero, Eds. (Kluwer, Dordrecht, Netherlands, 2005), pp. 149–168.
22. R. C. D. L. Hartman *et al.*, *Astrophys. J. Suppl. Ser.* **123**, 79 (1999).
23. B. Aschenbach, *Nature* **396**, 141 (1998).
24. F. Aharonian *et al.*, *Astron. Astrophys.* **437**, L7 (2005).
25. O. C. de Jager, A. K. Harding, P. Sreekumar, M. Strickman, *Astron. Astrophys.* **120** (suppl.), 441 (1996).
26. P. A. Caraveo, A. De Luca, R. P. Mignani, G. F. Bignami, *Astrophys. J.* **561**, 930 (2001).
27. H. Alvarez, J. Aparici, J. May, P. Reich, *Astron. Astrophys.* **372**, 636 (2001).
28. A. S. Hales *et al.*, *Astrophys. J.* **613**, 977 (2004).
29. The stellar radiation field peak is generally assumed at $E \approx 1$ eV, well fitting the gamma-ray galactic diffuse emission; see, e.g., www.iasf-milano.inaf.it/~giuliani/public/thesis/node10.html.
30. F. Mattana *et al.*, *Astrophys. J.* **694**, 12 (2009).
31. C. Pittori *et al.*, *Astron. Astrophys.* **506**, 1563 (2009).
32. A. Abdo *et al.*, *Astrophys. J. Suppl. Ser.* **183**, 46 (2009).
33. A. Pellizzoni *et al.*, *AIP Conference Proceedings*, vol. 745, F. A. Aharonian, H. J. Voelk, D. Horns, Eds. (2nd International Symposium on High Energy Gamma-Ray Astronomy, Heidelberg) (American Institute of Physics, New York, 2005), pp. 371–376.

34. The AGILE mission is funded by the Italian Space Agency with scientific and programmatic participation by the Italian Institute of Astrophysics and the Italian Institute of Nuclear Physics.

Supporting Online Material
www.sciencemag.org/cgi/content/full/science.1183844/DC1
SOM Text
Figs. S1 and S2
References

26 October 2009; accepted 15 December 2009
Published online 31 December 2009;
10.1126/science.1183844
Include this information when citing this paper.

Visualizing Critical Correlations Near the Metal-Insulator Transition in $Ga_{1-x}Mn_xAs$

Anthony Richardella,[1,2]* Pedram Roushan,[1]* Shawn Mack,[3] Brian Zhou,[1] David A. Huse,[1] David D. Awschalom,[3] Ali Yazdani[1]†

Electronic states in disordered conductors on the verge of localization are predicted to exhibit critical spatial characteristics indicative of the proximity to a metal-insulator phase transition. We used scanning tunneling microscopy to visualize electronic states in $Ga_{1-x}Mn_xAs$ samples close to this transition. Our measurements show that doping-induced disorder produces strong spatial variations in the local tunneling conductance across a wide range of energies. Near the Fermi energy, where spectroscopic signatures of electron-electron interaction are the most prominent, the electronic states exhibit a diverging spatial correlation length. Power-law decay of the spatial correlations is accompanied by log-normal distributions of the local density of states and multifractal spatial characteristics.

Since Anderson first proposed 50 years ago that disorder could localize electrons in solids (*1*), studies of the transition between extended and localized quantum states have been at the forefront of physics (*2*). Realizations of Anderson localization occur in a wide range of physical systems from seismic waves to ultracold atomic gases, in which localization has recently been achieved with random optical lattices (*3*). In electronic systems, the